BASIC RESEARCH www.jasn.org

The NLRP3 Inflammasome Promotes Renal Inflammation and Contributes to CKD

Akosua Vilaysane,* Justin Chun,* Mark E. Seamone,*‡ Wenjie Wang,* Rick Chin,* Simon Hirota,* Yan Li,* Sharon A. Clark,* Jurg Tschopp,† Kiril Trpkov,‡ Brenda R. Hemmelgarn,* Paul L. Beck,* and Daniel A. Muruve*

Departments of *Medicine and ‡Pathology, University of Calgary, Calgary, Alberta, Canada; and †Department of Biochemistry, University of Lausanne, Epalinges, Switzerland

ABSTRACT

Inflammation significantly contributes to the progression of chronic kidney disease (CKD). Inflammasome-dependent cytokines, such as IL-1β and IL-18, play a role in CKD, but their regulation during renal injury is unknown. Here, we analyzed the processing of caspase-1, IL-1β, and IL-18 after unilateral ureteral obstruction (UUO) in mice, which suggested activation of the Nlrp3 inflammasome during renal injury. Compared with wild-type mice, *Nlrp3*$^{-/-}$ mice had less tubular injury, inflammation, and fibrosis after UUO, associated with a reduction in caspase-1 activation and maturation of IL-1β and IL-18; these data confirm that the Nlrp3 inflammasome upregulates these cytokines in the kidney during injury. Bone marrow chimeras revealed that Nlrp3 mediates the injurious/inflammatory processes in both hematopoietic and nonhematopoietic cellular compartments. In tissue from human renal biopsies, a wide variety of nondiabetic kidney diseases exhibited increased expression of NLRP3 mRNA, which correlated with renal function. Taken together, these results strongly support a role for NLRP3 in renal injury and identify the inflammasome as a possible therapeutic target in the treatment of patients with progressive CKD.

J Am Soc Nephrol 21: 1732–1744, 2010. doi: 10.1681/ASN.2010020143

Chronic kidney disease (CKD) is a significant cause of morbidity and mortality in the general population.[1,2] In nondiabetic CKD, the progression from mild/moderate kidney disease to ESRD is a complex process that involves many factors, including tubulointerstitial inflammation and fibrosis. The involvement of mononuclear inflammatory cells in the damaged renal interstitium is a universal finding in failing kidneys and correlates inversely with renal function.[3–9] The molecular mechanisms that regulate inflammation in CKD, however, remain unclear.

An inflammatory response is induced during cellular injury such as necrosis.[10] Cellular contents that are inappropriately released after loss of plasma membrane integrity are endogenous adjuvants or danger-associated molecular patterns (DAMPs).[11–13] These DAMPs alert the innate immune system to cellular injury and produce a proinflammatory response to aid the repair of damaged tissues. Although beneficial in the case of pathogens, the reaction to endogenous (nonmicrobial) injury can contribute to tissue damage and disease progression.

The NOD-like receptors (NLRs) compose a group of pattern recognition receptors involved in a wide variety of host innate immune responses to microbial and nonmicrobial stimuli.[14] The best understood members include NOD2 (NLRC2, implicated in Crohn's disease)[15] and NLRP3 (also known as NALP3 or cryopyrin). Upon activation,

Received February 3, 2010. Accepted May 25, 2010.

Published online ahead of print. Publication date available at www.jasn.org.

Correspondence: Dr. Daniel A. Muruve, Department of Medicine, University of Calgary, 3330 Hospital Drive NW, Calgary, AB, T2N 4N1 Canada. Phone: 403-220-2418; Fax: 403-210-3949; E-mail: dmuruve@ucalgary.ca

the NLRP3 proteins oligomerize and recruit *via* homotypic molecular interactions, the adaptor protein ASC (apoptosis-associated speck-like protein containing a caspase recruitment domain), and the protease caspase-1 to form a protein complex termed "the inflammasome."[16] The formation of the inflammasome induces caspase-1 autoprocessing and activation that results in the processing of cellular substrates including the cytokines pro-IL-1β and pro-IL-18.[17,18] In the case of IL-1β, caspase-1 cleaves the 35-kD pro-IL-1β to generate the mature and secreted 17-kD cytokine.

Recent reports have implicated the NLRP3 inflammasome in the recognition of endogenous danger signals released from damaged and dying cells. DAMPs capable of activating the NLRP3 inflammasome include reactive oxygen species, extracellular ATP, monosodium urate crystals, nucleic acids, and extracellular matrix components including hyaluronan and biglycan.[19–24] Consistent with these observations, the NLRP3 inflammasome has been implicated in the pathogenesis of various nonmicrobial diseases, including diabetes, gout, silicosis, and acetaminophen liver toxicity.[19,20,25,26] The coexistence of cellular injury and inflammation suggests that the NLRP3 inflammasome may also play a role in regulating inflammation in CKD. Furthermore, the NLRP3 agonist biglycan and cytokines such as IL-1β, IL-18, and the IL-1 receptor all contribute to renal inflammation and fibrosis.[24,27–30] In this study, we demonstrated that the Nlrp3 inflammasome regulates renal inflammation and fibrosis during unilateral ureteral obstruction (UUO) in mice. In addition, studies of humans demonstrated increased NLRP3 in a variety of nondiabetic kidney diseases and CKD. These data provide valuable insight into the processes driving renal inflammation and CKD progression and identify NLRP3 as a novel target for therapeutic intervention.

RESULTS

Inflammasome Activation in Mouse UUO

Markers of inflammasome activation include the posttranslational processing of caspase-1 and the proinflammatory cytokines IL-1β and IL-18.[16] To determine whether the inflammasome was activated in renal injury, we probed kidney lysates from C57Bl/6 mice by immunoblotting for mature IL-1β and IL-18 and activated caspase-1 at 3, 7, and 14 days after UUO (Figure 1A). Increasing amounts of cleaved IL-1β and IL-18 were observed in the lysates of ligated kidneys over a 14-day time course in obstructed but not sham-operated or contralateral kidneys. Consistent with the inflammatory response after ureteral obstruction, an increase in pro-IL-1β expression was also observed. It should be noted, however, that, unlike IL-1β processing, the upregulation of pro-IL-1β is dependent on signaling *via* NF-κB and not the inflammasome *per se*.[16] Consistent with cytokine maturation, caspase-1 activation also oc-

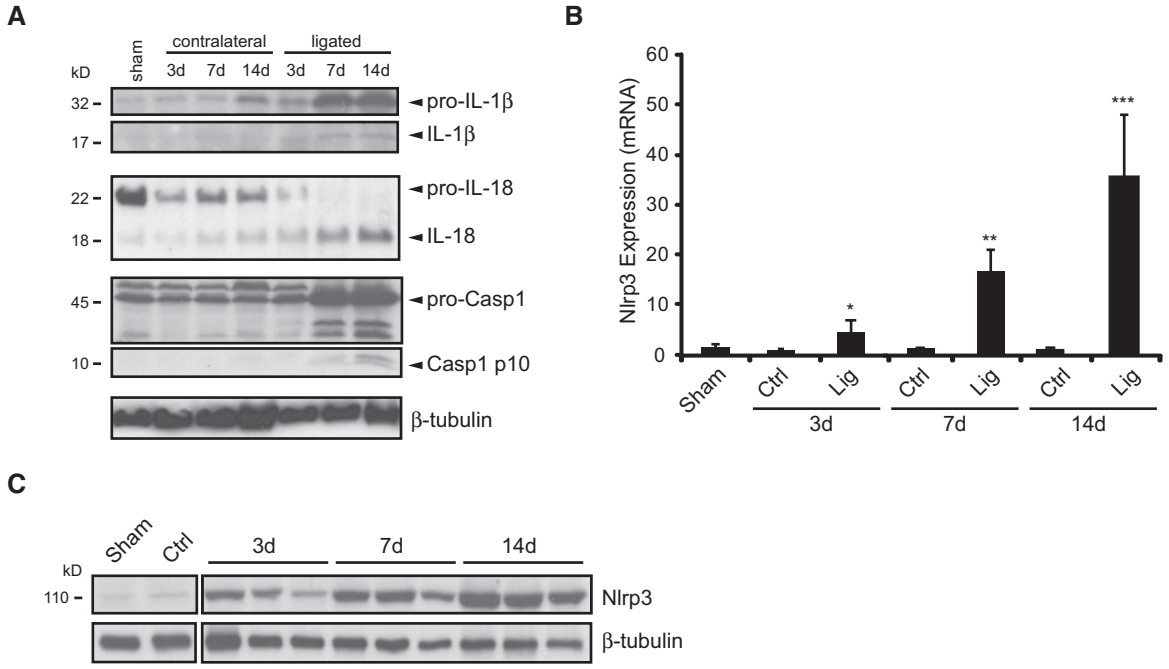

Figure 1. The inflammasome is activated in mice after UUO. (A) IL-1β, IL-18, and caspase-1 activation in mice after UUO. Immunoblotting of kidney tissue lysates from C57Bl/6 mice at 3, 7, and 14 days after UUO. Contralateral (Ctrl) and sham kidneys are used as controls. The appearance of mature (processed) IL-1β, IL-18, and the p10 subunit of active caspase-1 is observed in the ligated (Lig) kidneys at 7 to 14 days, consistent with inflammasome activation. (B) Nlrp3 mRNA expression in mice at 3, 7, and 14 days after UUO (quantitative real-time PCR, normalized to glyceraldehyde-3-phosphate dehydrogenase [GAPDH]). Data are mean ± SD Nlrp3 mRNA expression. $P < 0.001$, UUO *versus* sham, $n = 4$. (C) Nlrp3 protein expression in mouse kidney at 3, 7, and 14 days after UUO (immunoblotting).

curred in ligated kidneys, as demonstrated by the appearance of the p10 subunit at 7 and 14 days.

Nlrp3 has been implicated in the sensing of a variety of endogenous danger signals, such as uric acid, that are increased in CKD. To determine whether Nlrp3 played a role in chronic renal injury, we used real-time PCR and immunoblotting. Nlrp3 mRNA and protein expression increased progressively over a 14-day time course in comparison with the low baseline levels observed in contralateral and sham control kidneys (Figure 1, B and C).

Renal Pathology in *Nlrp3*$^{-/-}$ Mice after UUO

The previous results demonstrated strong evidence that the Nlrp3 inflammasome may play a role in renal injury. UUO induces significant tubulointerstitial inflammation and tubular injury within 14 days. To determine whether Nlrp3 contributed to this pathogenesis, we performed UUO in *Nlrp3*$^{-/-}$ mice. *Nlrp3*$^{+/+}$ and *Nlrp3*$^{+/-}$ littermates were used as controls. At 14 days after UUO, *Nlrp3*$^{-/-}$ mice displayed significantly less tubular injury as determined histologically and by pathologic scoring of tubular injury (Figure 2, A and B). Complete absence of *Nlrp3* was required because heterozygote littermates displayed similar pathologic features as *Nlrp3*$^{+/+}$ mice. Quantitative analysis of intact cortical tubular area corroborated the pathologic scoring and was consistently and significantly higher in *Nlrp3*$^{-/-}$ mice compared with heterozy-

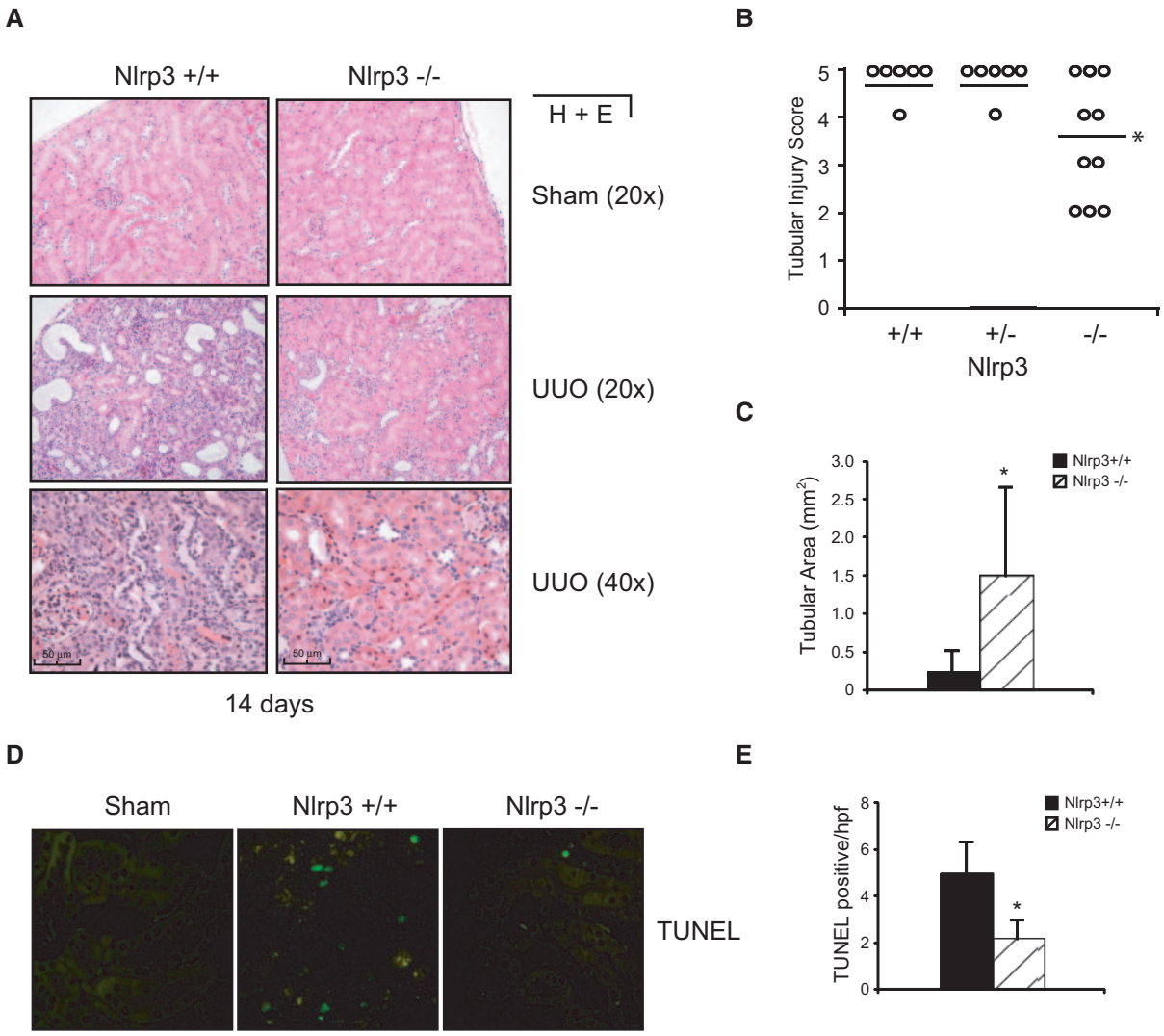

Figure 2. Nlrp3 contributes to tubular injury in mice undergoing UUO. (A) Histology (hematoxylin and eosin) of kidney sections from *Nlrp3*$^{+/+}$ and *Nlrp3*$^{-/-}$ mice after 14 days of UUO. (B) Tubular injury scoring in *Nlrp3*$^{+/+}$ ($n = 6$), *Nlrp3*$^{+/-}$ ($n = 6$), and *Nlrp3*$^{-/-}$ ($n = 10$) mice at 14 days after UUO (mean score, *Nlrp3*$^{+/+}$ *versus* *Nlrp3*$^{-/-}$ $P < 0.05$). (C) Quantification of intact cortical tubular area in *Nlrp3*$^{+/+}$ and *Nlrp3*$^{-/-}$ mice at 14 days after UUO (mean ± SD tubular area; $P < 0.05$, *Nlrp3*$^{+/+}$ *versus* *Nlrp3*$^{-/-}$; $n = 6$ to 10). (D) Immunofluorescence TUNEL staining of kidney sections from *Nlrp3*$^{+/+}$ and *Nlrp3*$^{-/-}$ mice. Sham *Nlrp3*$^{+/+}$ kidneys are shown as controls. (E) Quantification of TUNEL-positive cells in *Nlrp3*$^{+/+}$ and *Nlrp3*$^{-/-}$ kidney sections (mean ± SD cell number/high-power field; $P < 0.05$, *Nlrp3*$^{+/+}$ *versus* *Nlrp3*$^{-/-}$; $n = 4$).

gote and wild-type littermates (Figure 2C). Consistent with these observations, *Nlrp3*$^{-/-}$ mice displayed a general reduction in apoptosis in the kidney compared with *Nlrp3*$^{+/+}$ mice as determined by terminal deoxynucleotidyl transferase–mediated digoxigenin-deoxyuridine nick-end labeling (TUNEL) staining (Figure 2, D and E). Not surprising, by 4 weeks, tubular injury in *Nlrp3*$^{-/-}$ mice was similar to that in wild-type and heterozygote controls (data not shown).

Nlrp3$^{-/-}$ Mice Display Reduced Tubulointerstitial Inflammation after UUO

To determine whether the preserved tubular architecture was associated with a reduction in inflammation, we performed immunohistochemistry and cytokine analysis. Probing for the pan-leukocyte marker CD11b using immunohistochemistry, *Nlrp3*$^{-/-}$ displayed a significant reduction in leukocyte infiltration at 7 and 14 days after UUO compared with wild-type littermates (Figure 3A). Image analysis of CD11b staining confirmed a significant reduction in leukocyte infiltration area in *Nlrp3*$^{-/-}$ mice at 14 days (Figure 3B). The leukocyte population present within injured kidneys consisted primarily of F4/80-positive macrophages and to a lesser extent neutrophils, both of which were reduced in *Nlrp3*$^{-/-}$ mice at 14 days (Figure 3C). Consistent with the reduction in inflammatory infiltrates, expression of the chemokine CCL2 (monocyte chemoattractant protein-1) was significantly reduced in the kidneys of *Nlrp3*$^{-/-}$ mice after UUO at 7 and 14 days compared with wild-type controls (Figure 3D).

The generation of mature cytokines, such as IL-1β and IL-18, involves two separate processes: The induction of NF-κB–

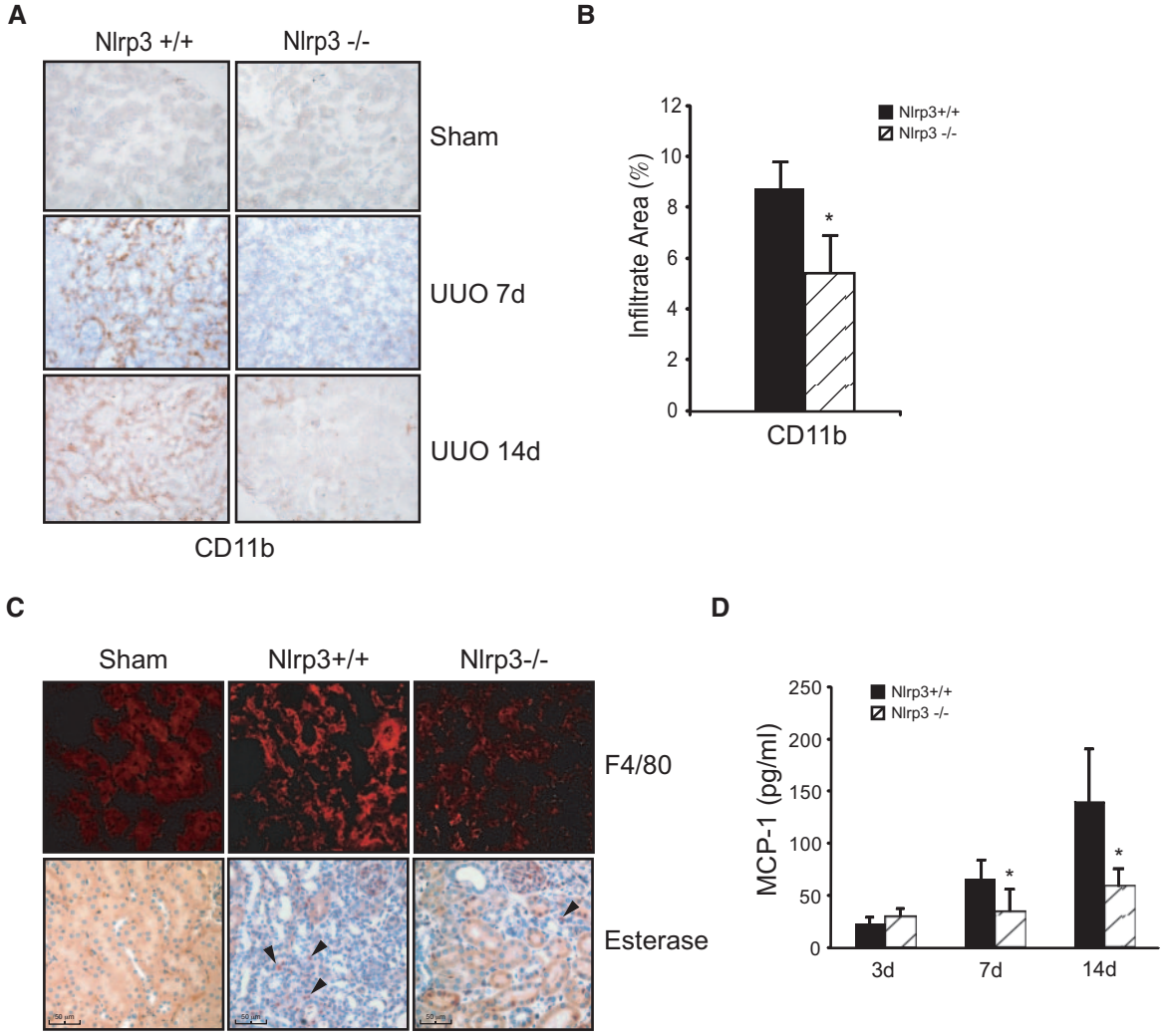

Figure 3. Renal inflammation is reduced in *Nlrp3*$^{-/-}$ mice after UUO. (A) Immunohistochemistry of kidney tissues with the leukocyte marker CD11b at days 7 and 14 after UUO in *Nlrp3*$^{+/+}$ and *Nlrp3*$^{-/-}$ mice. (B) Quantification of CD11b^{+} infiltrate area at 14 days after UUO (mean ± SD % area; $P < 0.05$, *Nlrp3*$^{+/+}$ *versus* *Nlrp3*$^{-/-}$; $n = 6$ *Nlrp3*$^{+/+}$ and 10 *Nlrp3*$^{-/-}$). (C) F4/80 immunofluorescence (macrophages) and esterase staining (granulocytes, examples marked with arrows) in *Nlrp3*$^{+/+}$ and *Nlrp3*$^{-/-}$ mouse kidneys at 14 days after UUO. Sham *Nlrp3*$^{+/+}$ kidneys are shown as controls. (D) CCL2 (monocyte chemoattractant protein-1) chemokine levels in mouse kidneys at 3, 7, and 14 days after UUO (immunobead assay, mean ± SD; $P < 0.05$, *Nlrp3*$^{+/+}$ *versus* *Nlrp3*$^{-/-}$; $n = 6$ to 10).

dependent mRNA expression and translation of the procytokine and inflammasome-dependent processing and release of the mature and active cytokine.[16] To determine whether inflammasome activity was reduced in *Nlrp3*$^{-/-}$ mice after UUO, we used immunoblotting to detect caspase-1, IL-1β, and IL-18 processing. Consistent with the role of the Nlrp3 inflammasome in this model of renal injury, at 14 days, *Nlrp3*$^{-/-}$ mice displayed less activated caspase-1 compared with wild-type controls as determined by immunoblotting for the active p10 subunit (Figure 4, A and B). Similarly, emergence of the mature 17-kD IL-1β and 18-kD IL-18 cytokines was also reduced at 7 days in *Nlrp3*$^{-/-}$ mice (Figure 4, C through F). At 14 days, differences in IL-1β and IL-18 maturation did not reach statistical significance (data not shown), suggesting the presence of redundant pathways. In this regard, mRNA of potential inflammasome-forming NLRs, Nlrp1b and Nlrp12, was increased after UUO at 14 days (Figure 5A). Furthermore, the expression of hyaluronan, high-mobility group box protein-1 (HMGB1), and biglycan (endogenous pro-inflammatory molecules that can activate TLR2 and TLR4[24,31]), although delayed in *Nlrp3*$^{-/-}$ mice at 3 and 7 days, was similar to wild-type controls by 14 days after UUO (Figure 5, B and C). Together, these data show that Nlrp3 is an essential mediator of the inflammatory response in the kidney after UUO, but redundant inflammatory pathways exist.

Nlrp3$^{-/-}$ Mice Display Reduced Tubulointerstitial Fibrosis after UUO

Inflammation is a critical factor in the development of renal fibrosis.[6] We next performed experiments to determine whether the reduction in inflammation in *Nlrp3*$^{-/-}$ mice resulted in less renal fibrosis. Masson trichrome staining and quantitative assessment confirmed that *Nlrp3*$^{-/-}$ kidneys showed a significant reduction in fibrosis at day 14 of UUO when compared with *Nlrp3*$^{+/+}$ kidneys (Figure 6, A and B). Consistent with these observations, loss of the epithelial cell marker E-cadherin was less profound in ligated *Nlrp3*$^{-/-}$ kidneys. Similarly, expression of the myofibroblast marker α-smooth muscle actin was significantly increased in *Nlrp3*$^{+/+}$ mice compared with *Nlrp3*$^{-/-}$ mice (Figure 6, C and D); therefore, *Nlrp3*$^{-/-}$ mice displayed less tubular injury, tubulointerstitial inflammation, and fibrosis

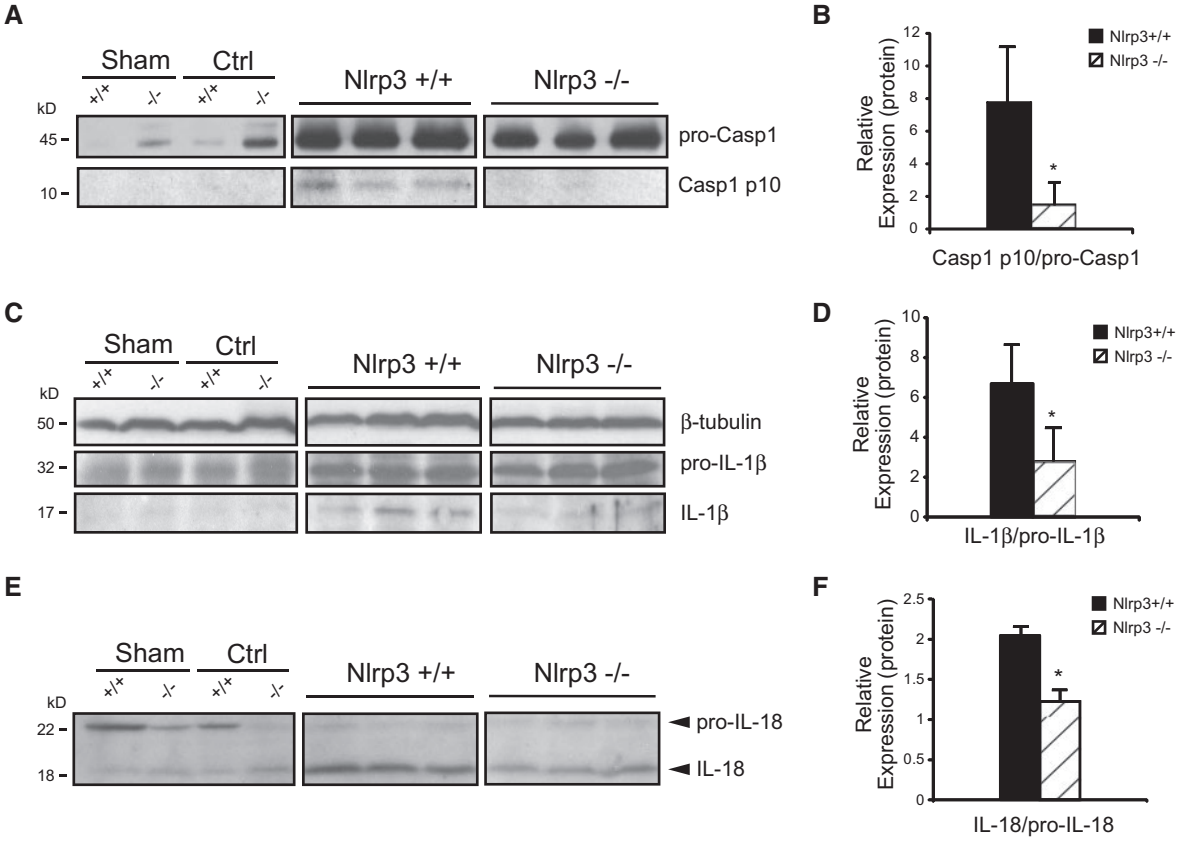

Figure 4. Renal cytokine maturation is reduced in *Nlrp3*$^{-/-}$ mice after UUO. (A) Caspase-1 immunoblotting in *Nlrp3*$^{+/+}$ and *Nlrp3*$^{-/-}$ mice at 14 days after UUO. Appearance of caspase-1 p10 subunit indicates activation. Sham and contralateral (Ctrl) kidneys are used as controls. (B) Quantification of processed caspase-1 normalized to pro-caspase-1 (mean ± SD; $P < 0.05$, *Nlrp3*$^{+/+}$ *versus* *Nlrp3*$^{-/-}$; $n = 6$ *Nlrp3*$^{+/+}$ and 10 *Nlrp3*$^{-/-}$). (C) IL-1β immunoblotting in *Nlrp3*$^{+/+}$ and *Nlrp3*$^{-/-}$ mice at 7 days after UUO. Appearance of mature 17-kD IL-1β indicates activation. (D) Quantification of processed IL-1β normalized to pro-IL-1β (mean ± SD; $P < 0.05$, *Nlrp3*$^{+/+}$ *versus* *Nlrp3*$^{-/-}$; $n = 6$). (E) IL-18 immunoblotting in *Nlrp3*$^{+/+}$ and *Nlrp3*$^{-/-}$ mice at 7 days after UUO. Appearance of mature 18-kD IL-18 indicates activation (F) Quantification of processed IL-18 normalized to pro-IL-18 (mean ± SD; $P < 0.05$, *Nlrp3*$^{+/+}$ *versus* *Nlrp3*$^{-/-}$; $n = 6$).

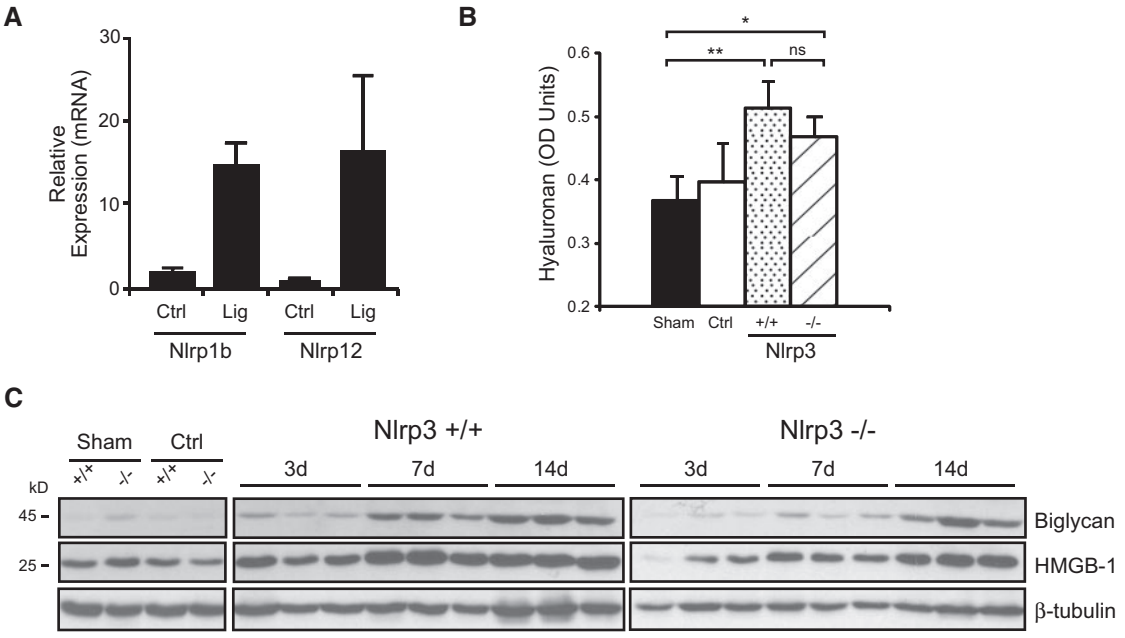

Figure 5. UUO activates redundant inflammatory pathways in mouse kidneys. (A) Nlrp1b and Nlrp12 mRNA expression (quantitative real time reverse transcriptase–PCR, normalized to GAPDH) in ligated (Lig) or contralateral (Ctrl) *Nlrp3*$^{+/+}$ mouse kidneys at 14 days after UUO. (B) Hyaluronan content (ELISA) in kidney lysates from *Nlrp3*$^{+/+}$ and *Nlrp3*$^{-/-}$ mice at 14 days after UUO (sham *versus* *Nlrp3*$^{+/+}$, $P < 0.01$, *versus* *Nlrp3*$^{-/-}$, $P < 0.05$; *Nlrp3*$^{+/+}$ *versus* *Nlrp3*$^{-/-}$, NS; $n = 5$) (C) Immunoblotting for biglycan and HMGB1 in kidney lysates from *Nlrp3*$^{+/+}$ and *Nlrp3*$^{-/-}$ mice at 3, 7, and 14 days after UUO. Fourteen-day sham and contralateral kidneys are used as controls.

after UUO, confirming an essential role for the Nlrp3 inflammasome in renal injury (Figure 6).

Cellular Compartments and Nlrp3 in UUO

The Nlrp3 inflammasome has been characterized primarily in leukocytes. To determine whether the reduction in injury after UUO in knockout mice was due to Nlrp3 deficiency in infiltrating leukocytes, we performed bone marrow (BM) chimera studies. Irradiated *Nlrp3*$^{-/-}$ and *Nlrp3*$^{+/+}$ mice were reconstituted with either *Nlrp3*$^{+/+}$ or *Nlrp3*$^{-/-}$ BM cells. After recovery from the BM transplants at 6 weeks, mice underwent UUO and kidneys were analyzed at 14 days after the surgery. *Nlrp3*$^{+/+}$ to *Nlrp3*$^{+/+}$, *Nlrp3*$^{+/+}$ to *Nlrp3*$^{-/-}$, and *Nlrp3*$^{-/-}$ to *Nlrp3*$^{+/+}$ BM chimeras all showed significant tubular injury as determined by histology, quantitative analysis of intact cortical tubular area, and loss of E-cadherin expression (Figure 7). In addition, these chimeras displayed similar levels of processed IL-18, consistent with inflammasome activation. In contrast, *Nlrp3* $^{-/-}$ to *Nlrp3*$^{-/-}$ chimeras showed less tubular injury, increased E-cadherin expression, and a trend ($P = 0.11$) toward less IL-18 processing in the kidneys, consistent with the phenotype of nonchimeric *Nlrp3*$^{-/-}$ mice at 14 days after UUO.

These data suggested that Nlrp3 has a biological function in both hematopoietic and renal compartments during renal injury. Consistent with this premise, Nlrp3 mRNA and protein expression was clearly detected at baseline and induced by LPS and phorbol-12-myristate-13-acetate (PMA) in primary tubular epithelial cells (TEC) isolated from *Nlrp3*$^{+/+}$ mice and human kidneys respectively (Figure 8, A and B). Using TECs isolated from *Nlrp3*$^{+/+}$ and *Nlrp3*$^{-/-}$ mice, we were unable to show consistently a role for Nlrp3 in H_2O_2-induced necrosis (Figure 8E) or IL-1β/IL-18 processing; however, pro-IL-1β and pro-IL-18 expression levels were very low, despite LPS priming in these cells (data not shown). Conversely, cyclohexamide/TNF-α–induced apoptosis[32] was significantly reduced in *Nlrp3*$^{-/-}$ TECs as determined by cleavage of the caspase-3 substrate poly(ADP-ribose) polymerase-1[33] (Figure 8, C and D), confirming a biological role for Nlrp3 in renal tubular epithelium.

NLRP3 mRNA Expression in Human Nondiabetic Kidney Disease

To determine whether NLRP3 was expressed in human kidney disease, we analyzed kidney biopsies by quantitative real-time PCR for NLRP3 mRNA expression. Biopsies from 43 patients with nondiabetic kidney disease were randomly chosen for analysis from the frozen renal tissue bank at Calgary Lab Services and the Department of Pathology, University of Calgary. Studied renal diseases included IgA nephropathy ($n = 9$), minimal change disease ($n = 3$); membranous glomerulopathy ($n = 3$), lupus nephritis ($n = 3$), secondary FSGS ($n = 9$), and hypertension/vascular nephrosclerosis ($n = 4$). In addition to patients with glomerular and nonglomerular CKD, several cases of acute kidney disease such as crescentic glomerulonephritis ($n = 5$) and acute tubular necrosis (ATN; $n = 7$) were included in the cohort for comparative purposes. Normal ne-

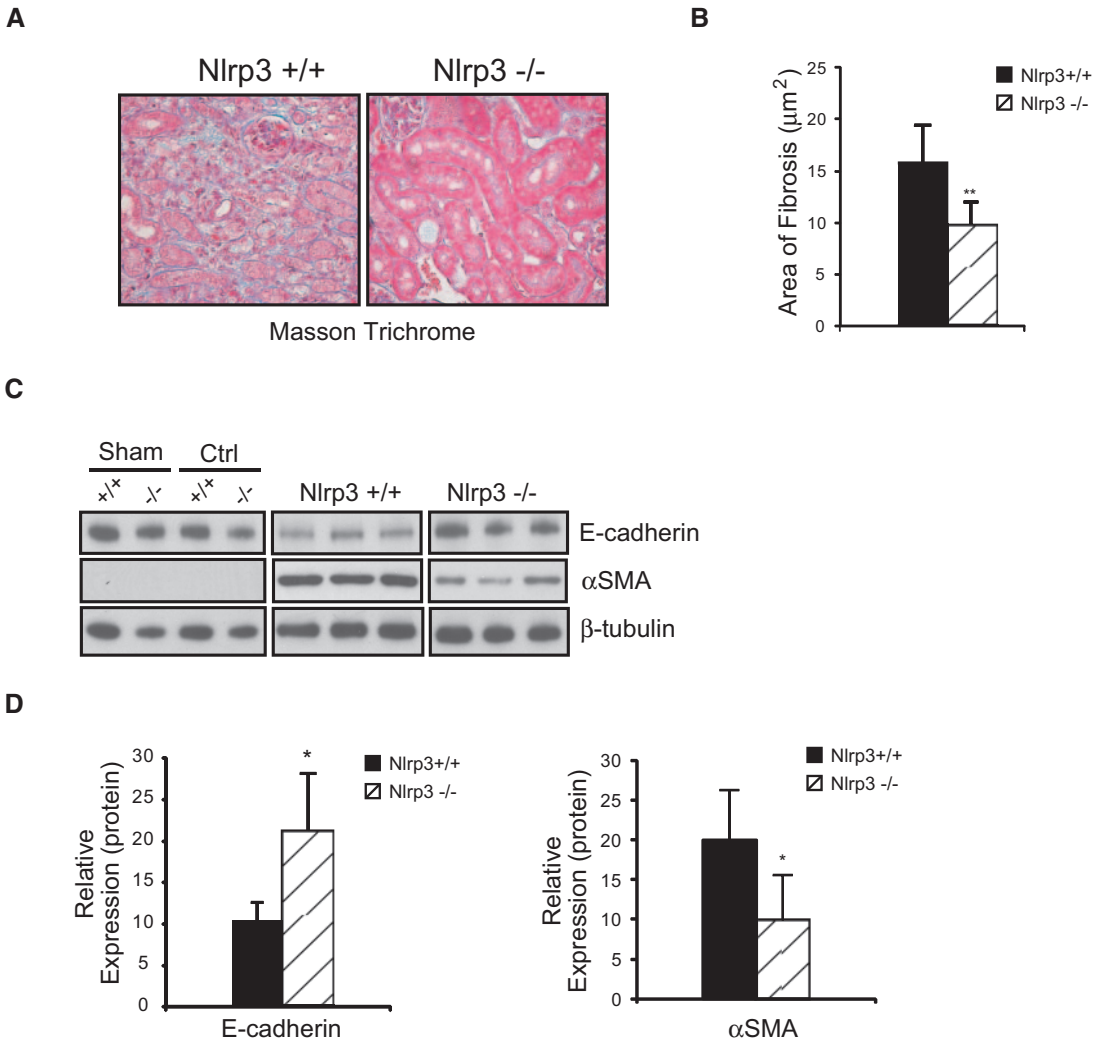

Figure 6. Renal fibrosis is reduced in *Nlrp3*$^{-/-}$ mice after UUO. (A) Masson trichrome staining on *Nlrp3*$^{+/+}$ and *Nlrp3*$^{-/-}$ kidneys at 14 days after UUO. (B) Quantification of renal fibrosis area at 14 days (mean ± SD area; $P < 0.01$, *Nlrp3*$^{+/+}$ *versus* *Nlrp3*$^{-/-}$; $n = 6$ *Nlrp3*$^{+/+}$ and 10 *Nlrp3*$^{-/-}$). (C) E-cadherin and α-smooth muscle actin (αSMA) expression in *Nlrp3*$^{+/+}$ and *Nlrp3*$^{-/-}$ kidneys at 14 days after UUO (immunoblotting). Fourteen-day sham and contralateral (Ctrl) kidneys are used as controls. (D) Quantification of E-cadherin and αSMA expression in *Nlrp3*$^{+/+}$ and *Nlrp3*$^{-/-}$ mice at 14 days normalized to β-tubulin (mean ± SD; $P < 0.05$, *Nlrp3*$^{+/+}$ *versus* *Nlrp3*$^{-/-}$; $n = 6$ to 10).

phrectomy samples were used as controls ($n = 16$). In normal kidneys, very little NLRP3 was expressed (Figure 9A). In comparison, NLRP3 expression was significantly increased in patients with acute kidney disease and CKD. In a subgroup analysis based on diagnosis, NLRP3 was found to be significantly increased over normal controls in all study groups (Figure 9A). Of the 43 patients, clinical renal function data within 6 months of biopsy was available for 37 through the Alberta Kidney Disease Network (AKDN) database[34] and correlated to NLRP3 expression. Patients with advanced renal failure (creatinine >300 μmol/L; $n = 4$) were excluded from the analysis to avoid patients with ESRD. The mean serum creatinine among the 33 patients was 121.9 ± 58.6 μmol/L. There was a statistically significant positive correlation between log NLRP3 expression in the kidney and serum creatinine ($r = 0.51$, $P < 0.01$; Figure 9B). On the basis of the experimental and human data, our results suggest that the NLRP3 inflammasome plays a significant role in renal injury and disease.

DISCUSSION

The NLRP3 inflammasome is an innate proteolytic complex that is known to be activated by a variety of nonmicrobial danger signals; therefore, it is an attractive candidate as a mediator of the inflammatory component observed in CKD. In this study, we show that NLRP3 plays a role in experimental and human CKD. Our data demonstrate that *Nlrp3*$^{-/-}$ mice display attenuated renal injury and fibrosis after 14 days of UUO. Moreover, our studies of human biopsies suggest a role

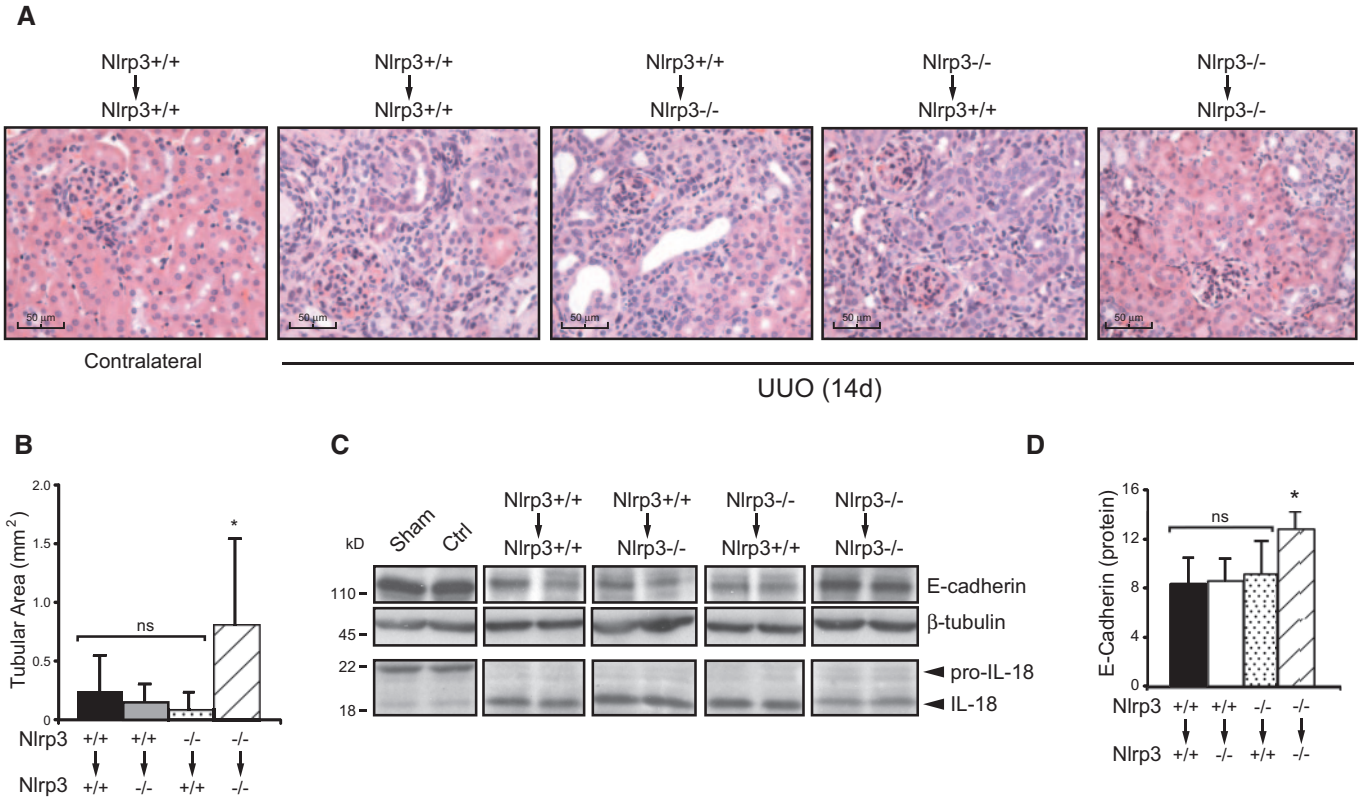

Figure 7. UUO in bone marrow chimeric mice show that Nlrp3 mediates renal injury from renal cells and infiltrating leukocytes. (A) Histology (hematoxylin and eosin) of kidney sections from Nlrp3 BM chimeric mice after 14 days of UUO. Contralateral kidney is from an $Nlrp3^{+/+}$ to $Nlrp3^{+/+}$ mouse. (B) Quantification of intact cortical tubular area in Nlrp3 BM chimeric mice at 14 days after UUO (mean ± SD tubular area; $Nlrp3^{+/+}$ to $Nlrp3^{+/+}$ [$n = 5$]), $Nlrp3^{+/+}$ to $Nlrp3^{-/-}$ [$n = 5$] and $Nlrp3^{-/-}$ to $Nlrp3^{+/+}$ [$n = 12$; NS]; all groups *versus* $Nlrp3^{-/-}$ to $Nlrp3^{-/-}$ [$n = 8$; $P < 0.05$]). (C) E-cadherin and IL-18 expression in kidneys of Nlrp3 BM chimeric mice at 14 days after UUO (immunoblotting). Sham and contralateral (Ctrl) kidney samples shown are from $Nlrp3^{+/+}$ to $Nlrp3^{+/+}$ mice. (D) Quantification of E-cadherin expression in Nlrp3 chimeras at 14 days normalized to β-tubulin (mean ± SD; $Nlrp3^{+/+}$ to $Nlrp3^{+/+}$, $Nlrp3^{+/+}$ to $Nlrp3^{-/-}$, and $Nlrp3^{-/-}$ to $Nlrp3^{+/+}$ [NS]; all groups *versus* $Nlrp3^{-/-}$ to $Nlrp3^{-/-}$ [$P < 0.05$]). Magnification, ×40.

for NLRP3 in both acute and chronic nondiabetic kidney disease. Together, these results identify NLRP3 and the inflammasome as a potential therapeutic target for a variety of nondiabetic kidney diseases and CKD.

Nonmicrobial (sterile) inflammation is an important component of many acute and chronic renal diseases.[6] Given its central role in the innate immune system and inflammation, it is not surprising that NLRP3 upregulation was observed in both murine renal injury and a variety of human nondiabetic CKDs. Our studies also demonstrate increased NLRP3 expression in acute kidney diseases such as crescentic glomerulonephritis and ATN, the latter in keeping with a recent study demonstrating a role for the Nlrp3 inflammasome in experimental renal ischemia-reperfusion injury.[35] In this study, we linked NLRP3 mRNA expression to the AKDN clinical database *via* a common patient-identifying code[34] and demonstrated a significant positive correlation between NLRP3 and kidney function. These data not only suggest that NLRP3 plays an important role in the pathogenesis of human kidney disease but also highlights a robust technique that allows rapid clinical translation of basic science data *via* the AKDN. Expansion of our data set and linkage to the AKDN in future studies will aid in further assessment of the clinical importance of NLRP3 in human kidney disease.

The generation of mature cytokines, such as IL-1β and IL-18, involves two separate processes: The induction of NF-κB–dependent mRNA expression and translation of the pro-cytokine and the inflammasome-dependent processing and release of the mature and active cytokine.[16] Inflammasome activity was present in the UUO model of renal injury as indicated by the appearance of cleaved IL-1β and IL-18 and active caspase-1 subunits. The absence of Nlrp3 resulted in the attenuation of tubular injury, reduced leukocyte infiltration, and renal fibrosis. Because IL-1β and IL-18 have been implicated in renal injury and fibrosis, reduced inflammasome-dependent cytokine maturation likely contributed to the improved phenotype observed in $Nlrp3^{-/-}$ mice. IL-1β, IL-18, and caspase-1 maturation were not completely suppressed in $Nlrp3^{-/-}$ mice, however. The upregulation of several TLR-activating ligands as well as potential inflammasome-forming Nlrp1b and Nlrp12 genes suggest that redundant inflammatory pathways contribute to the UUO phenotype.

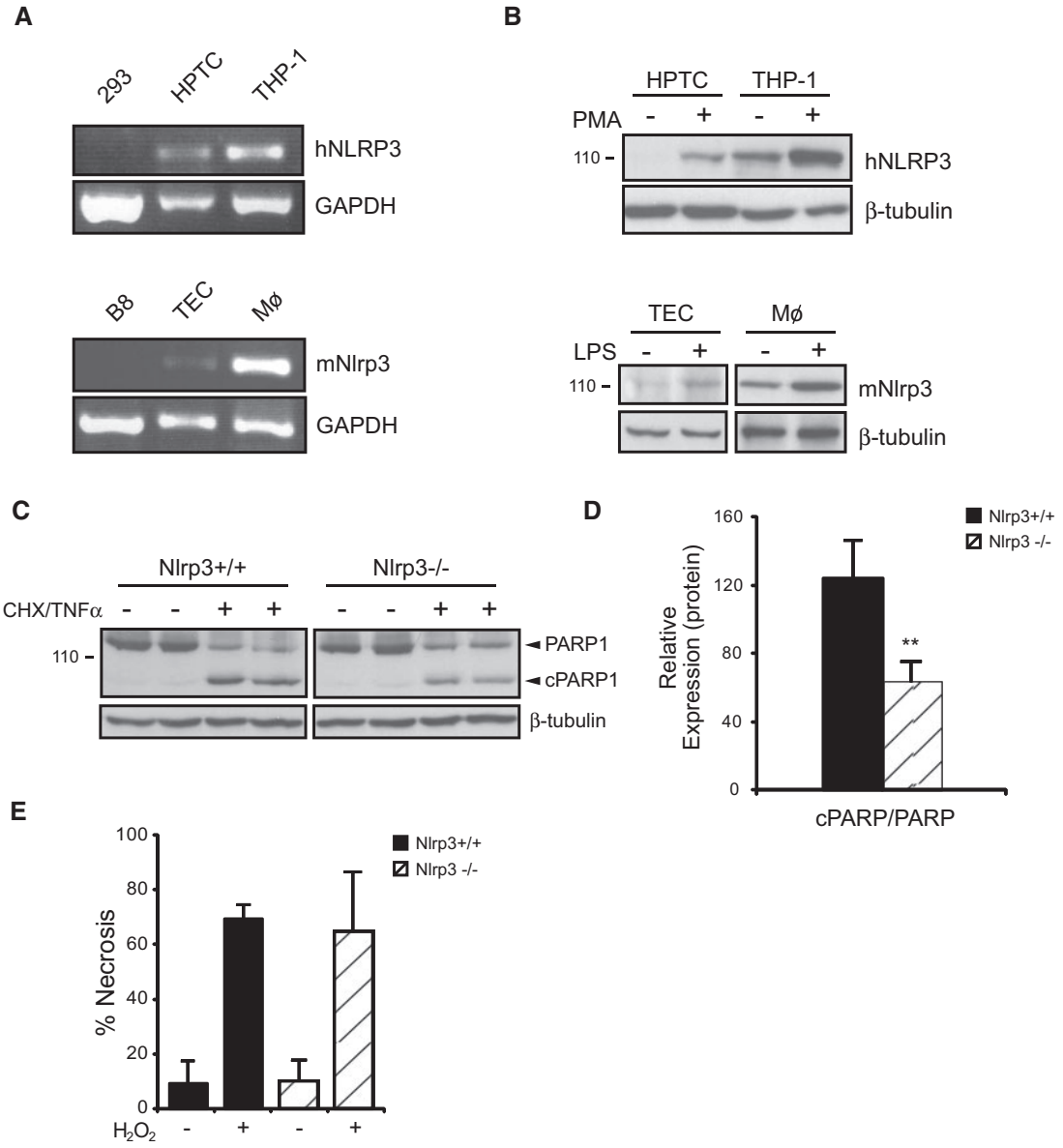

Figure 8. NLRP3 is expressed in primary renal TECs and contributes to apoptosis. (A) Semiquantitative reverse transcriptase–PCR for human and mouse NLRP3 mRNA in HEK293, primary human proximal tubular cells (HPTCs), THP-1 monocyte/macrophages, mouse B8 cells, primary C57Bl/6 TECs, and primary mouse BM macrophages. (B) Immunoblotting for NLRP3 in PMA-stimulated HPTCs and THP-1 monocyte/macrophages. Immunoblotting for mouse Nlrp3 in LPS-stimulated primary C57Bl/6 TECs and primary mouse BM macrophages. (C) Immunoblotting for poly(ADP-ribose) polymerase-1 (PARP1) cleavage (cPARP1) in *Nlrp3*$^{+/+}$ and *Nlrp3*$^{-/-}$ primary TECs induced to undergo apoptosis with cyclohexamide and TNF-α. (D) Quantification of cPARP1 normalized to total PARP1 in *Nlrp3*$^{+/+}$ and *Nlrp3*$^{-/-}$ primary TECs induced to undergo apoptosis (mean ± SD; $P < 0.01$, *Nlrp3*$^{+/+}$ *versus* *Nlrp3*$^{-/-}$; $n = 9$). (E) Flow cytometry (propidium iodide) of primary TECs after H_2O_2-induced necrosis (mean ± SD % propidium iodide–positive cells; NS, *Nlrp3*$^{+/+}$ *versus* *Nlrp3*$^{-/-}$; $n = 3$).

Our chimera and *in vitro* studies support a role for Nlrp3 in both hematopoietic and nonhematopoietic cellular compartments in the kidney. Nlrp3 inflammasome activation depends on an NF-κB–dependent priming step in which increased expression of Nlrp3 is required before ligand activation.[36] In this study, we show inducible Nlrp3 mRNA/protein expression in the ligated kidneys of mice as well as in TECs *in vitro*. Although the majority of studies focus on the role of Nlrp3 in leukocytes, our results show that Nlrp3 induction in renal tubular cells is required for apoptosis and suggest that the effects of the Nlrp3 inflammasome likely go beyond simple cytokine processing. Numerous potential substrates of the Nlrp3 inflammasome that could affect other cellular pathways such as glycolysis that are involved in cellular stress exist.[37] Future studies are required to elucidate fully the noncanonical Nlrp3 effects in TECs.

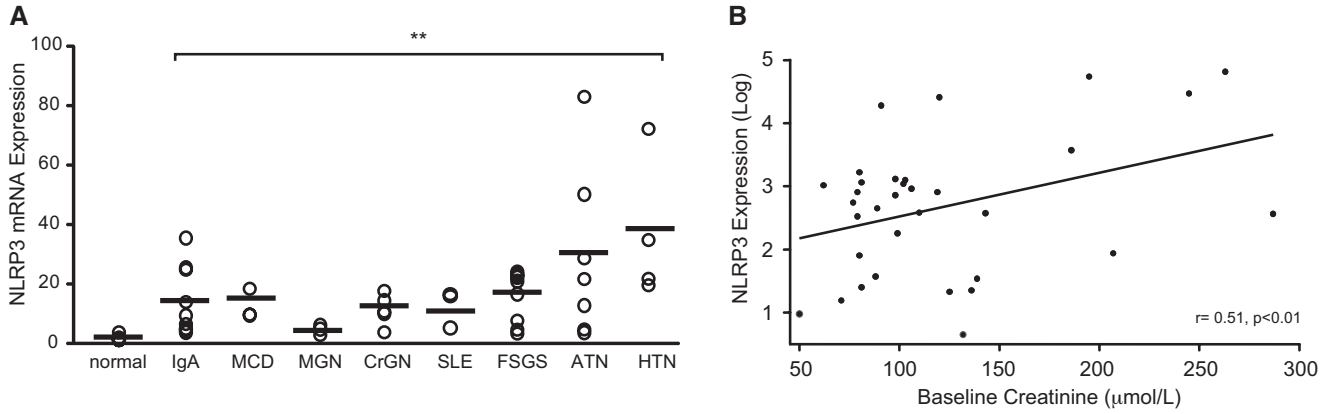

Figure 9. NLRP3 mRNA is expressed in human nondiabetic kidney disease. RNA is isolated from renal biopsies of patients with nondiabetic kidney disease. Normal $n = 16$; IgA nephropathy (IgA) $n = 9$; minimal change disease (MCD) $n = 3$; membranous glomerulonephritis (MGN) $n = 3$; crescentic GN (CrGN) $n = 5$; lupus nephritis (SLE) $n = 3$; secondary FSGS $n = 9$; ATN $n = 7$; hypertension/vascular nephrosclerosis (HTN) $n = 4$. (A) NLRP3 mRNA expression is assessed by quantitative real-time PCR. Values are normalized to endogenous 18S mRNA expression levels (mean NLRP3 mRNA expression, normal *versus* disease, all $P < 0.01$). (B) Scatter plot of NLRP3 mRNA expression (log) against renal function (creatinine, μmol/L) in patients with nondiabetic kidney disease ($r = 0.51$, $P < 0.01$; $n = 33$).

Our findings support the prevailing notion that the NLRP3 inflammasome functions as a general sensor of cell injury that results in a host inflammatory response. Renal tubular cell injury occurs as a result of a variety of insults, including ischemia, obstruction, and immune-mediated mechanisms,[38] that can result in the release of endogenous cellular components capable of activating the NLRP3 inflammasome.[16] For example, ATP in the mitochondrial fraction of necrotic cells activates the Nlrp3 inflammasome *via* $P2X_7$ receptors.[15,22,35,39] Consistent with these data, $P2X_7^{-/-}$ mice exhibit less tubular injury as well as reduced inflammation and fibrosis after UUO compared with their wild-type counterparts.[40] In addition to ATP, other cellular factors have also been shown to activate the NLRP3 inflammasome and play a role in CKD, including extracellular matrix components biglycan, hyaluronan, and uric acid crystals.[23,24,41] The ability of the NLRP3 inflammasome to respond to a variety of endogenous danger signals *via* a single common pathway makes it an attractive therapeutic target for kidney disease, including progressive CKD.

Specific therapies targeting CKD progression are few in number. Inflammation is undoubtedly an important component of CKD. Our characterization of the Nlrp3 inflammasome in human and experimental kidney disease sheds new light on the pathogenesis of CKD and also supports a role for NLRP3 in acute renal syndromes such as glomerulonephritis and ATN. Therapies designed to target the activation of the NLRP3 inflammasome or block its downstream effectors may prove useful in the treatment of progressive CKD and other common kidney diseases.

CONCISE METHODS

Animal Studies

$Nlrp3^{-/-}$ mice on a C57Bl/6[20] background, wild-type, and heterozygote littermates were bred and housed in a pathogen-free facility. Healthy 6- to 8-week-old male mice underwent left UUO or sham surgery as described previously.[42] Mice were anesthetized using intraperitoneal injection of a mixture of ketamine (125 mg/kg) and xylazine (12.5 mg/kg); recovered under a warming lamp; and received analgesia, standard food, and water for the duration of the experiment.

For chimera studies, BM cells were isolated from 4- to 6-week-old female $Nlrp3^{-/-}$ and $Nlrp3^{+/+}$ as described previously.[43] Recipient male mice were irradiated by Gammacell 1000 (Nordion Int., Kanata, Ontario, Canada) (^{137}Cs source) twice, at a dosage of 5.0 Gy, 3 hours apart. After the second irradiation, 10 to 20 $\times$ 10^6 donor BM cells were injected into recipients *via* the tail vein. For the first 2 weeks after BM transplantation, mice received 0.2% neomycin sulfate in their drinking water. UUO was performed at 6 weeks after the engraftment recovery period. Previously, we showed that this protocol produces complete engraftment using both flow cytometry (thy 1.1 to 1.2) and Y chromosome *in situ* hybridization.[43] All experimental procedures were conducted with the approval of the Animal Care Committee at the University of Calgary.

Tissue Preparation

After 3, 7, or 14 days of UUO, mice were killed and the kidneys were removed. Kidneys were flash-frozen or prepared for histology using 10% buffered formalin fixation. Flash-frozen samples were stored in OCT compound at −80°C. Tissue protein lysates were prepared by weighing frozen tissue and placing the samples in an appropriate amount of lysis buffer (10 mM Tris [pH 7.5], 1% NP-40, and 150 mM NaCl) complete with protease inhibitors. Tissue homogenization was achieved with a handheld homogenizer (Kimble Kontes). Protein concentrations were determined using the Bradford protein assay.

Immunoblotting, Immunobead Assays, and ELISA

Protein samples were separated on either 8 or 15% SDS-PAGE gels. Gels were transferred to nitrocellulose membranes and blocked with 5% milk proteins. Membranes were incubated at 4°C overnight with

primary antibodies as follows: Goat anti-mouse IL-18 (Santa Cruz Biotechnology), sheep anti-mouse IL-1β (Dr. Jurg Tschopp), mouse anti–E-cadherin (clone 36; BD Biosciences), rabbit anti-mouse caspase-1 (Santa Cruz Biotechnology), anti-mouse α-smooth muscle actin (Clone 1A4; Sigma), mouse anti-human NLRP3 (clone Cryo-2; Adipogen), rabbit anti-human biglycan (Abcam), rabbit anti-human HMGB1 (Cell Signaling), rabbit anti-human poly(ADP-ribose) polymerase-1 (Cell Signaling), and mouse anti–β-tubulin (clone D66; Sigma). Blots were washed, incubated with secondary horseradish peroxidase–conjugated antibodies as appropriate, and developed using ECL Western blotting detection reagents (Amersham, GE Healthcare). Protein expression was quantified using the Fluor-S-Multi Imager (BioRad) and Quantity One 4.2.3 software. The signal intensity of the bands of interest was normalized to the signal intensity of the corresponding β-tubulin, procaspase-1, pro-IL-1β, or pro-IL-18 band present on the same membrane.

Mouse kidney lysates (100 μg of protein) were analyzed for monocyte chemoattractant protein-1 chemokine levels using multiplex bead immunoassays as per the manufacturer's protocol (Luminex, Invitrogen). Plates were read using a Luminex 200 instrument, and data were analyzed with StarStation 2.3 software.

For hyaluronan ELISA, 50 μg of kidney protein lysates was used to coat a 96-well plate overnight at 4°C. After washing with PBS/0.1% Tween, samples were blocked with 10% BSA, followed by avidin and biotin. Samples were incubated with biotinylated hyaluronan-binding protein (Calbiochem) at room temperature for 1 hour, washed, and then incubated with avidin–horseradish peroxidase. 2,2′-Azinobis(3-ethylbenzthiazoline-6-sulfonic acid) was used as substrate, and absorbance was read at 405 nm.

Cell Culture

Primary mouse TECs were isolated from the kidneys of *Nlrp3*$^{+/+}$ and *Nlrp3*$^{-/-}$ mice as described previously.[42] TECs were established on a substratum of type IV collagen (human placenta; Sigma) and maintained in DMEM/F12 containing 10% FCS, 1% penicillin-streptomycin, 125 ng/ml prostaglandin E1 (Calbiochem), 25 ng/ml EGF (Sigma), 1.8 μg/ml l-thyroxine (Sigma), 3.38 ng/ml hydrocortisone, and 2.5 mg/ml insulin-transferrin-sodium selenite supplement (Sigma). Cells were used at less than passage 5. Human proximal TECs were isolated from normal human nephrectomy samples. Cells were cultured as per mouse TEC with the exception that human EGF was used in the culture medium. Epithelial phenotype for all renal cells was confirmed by immunohistochemistry for E-cadherin, Zona occludens-1, and the proximal tubule cell enzyme c-glutamyl transpeptidase as described previously[42] (data not shown). Human embryonic kidney cells (HEK293 cells) and mouse B8 astrocytoma cells were maintained in DMEM containing 10% FBS and 1% penicillin-streptomycin. Human THP-1 monocytic leukemia cells were grown in RPMI 1640 medium supplemented with 10% FBS, 1% penicillin-streptomycin, 1% MEM sodium pyruvate (100 mM), and 0.01% β-mercaptoethanol.

For *in vitro* studies, cells were primed with ultrapure LPS (200 ng/ml; Invivogen) or PMA (80 nM) for 24 hours before immunoblotting to induce NLRP3 expression. For inducing apoptosis, TECs were serum-starved and primed simultaneously for 24 hours using either PMA or ultrapure LPS in serum-free K1 medium. Apoptosis was induced for 24 hours with 100 ng/ml mouse TNF-α (Sigma) and 5 μg/ml cyclohexamide (Sigma). For inducing necrosis, primed TECs were treated with 10 mM H_2O_2 (Sigma-Aldrich) in serum-free medium for 3 hours at 37°C. Cells were harvested and analyzed for cell viability using propidium iodide (Sigma) and flow cytometry.

Quantitative Real-Time and Semiquantitative PCR

RNA was isolated from cells or frozen mouse kidney tissue with the RNeasy Mini kit (Qiagen) as per the manufacturer's instructions. For mouse samples, reverse transcription was carried out using 500 ng of RNA, random hexamers (3 μg/μl), and M-MLV reverse transcriptase (200 U/μl; Invitrogen) as per the manufacturer's protocol. Real-time PCR primers and probes were designed using Primer3 software (Applied Biosystems) to amplify sequence fragments of the murine Nlrp1b, Nlrp3, and Nlrp12 genes: Nlrp1b forward 5′-GACTTTGTGGCTTGTTGAATGC-3′ and reverse 5′-CATTTAGCTGCAGGTCTAGCTCTCT-3′; Nlrp3 forward 5′-AGAGCCTACAGTTGGGTGAAATG-3′, probe 6-FAM-5′-CGTGCCTTAGAAGCG-3′-MGB, and reverse 5′-CCACGCCTACCAGGAAATCTC-3′; and Nlrp12 forward 5′-AGCGTGGTATATCCCTCGAAGA-3′ and reverse 5′-CCCTGAGCATCATGGAAAGAA-3′. Nlrp1b and Nlrp12 amplifications were performed using SYBR green chemistry. 20X Mouse GAPDH-FAM/MGB Probe (Applied Biosystems) was used as the endogenous control. Target gene reactions were formed in a total reaction volume of 25 μl using 12.5 μl of 2× Taqman Universal PCR Master Mix (Applied Biosystems), 900 nM of each primer, 200 nM probe, 2.95 μl of RNase/DNase-free distilled water, and 5 μl of cDNA template (diluted 1:5 from original). Amplification was performed in MicroAmp Fast Optical 96-well reaction plates (Applied Biosystems) using the 7900HT Fast Real-Time PCR System (Applied Biosystems), and results were analyzed with SDS 2.3 and RQ Manager software. Results were normalized to glyceraldehyde-3-phosphate dehydrogenase transcripts.

For the analysis of human NLRP3 mRNA expression, total RNA was extracted from frozen human kidney biopsy samples obtained from the frozen renal tissue bank at Calgary Lab Services and the Department of Pathology. Tissue samples from human kidney biopsies were homogenized using polypropylene pellet pestles with a hand-held homogenizer (Kimble Kontes) in microcentrifuge tubes. Total RNA from tissue was isolated using QIAshredder (Qiagen) tubes and an RNeasy Mini Kit (Qiagen) according to the manufacturer's protocol. Ten to 50 ng of RNA was used in reverse transcription reactions as described already. The sequences for human NLRP3 primers and probe were as follows: Forward primer 5′-TGAAGAAAGATTACCGTAAGAAGTACAGA-3′, reverse primer 5′-GCGTTTGTTGAGGCTCACACT-3′, and probe 6-FAM-5′-AATGCCCGTCTGGGTG-3′-MGB (Applied Biosystems). The 20× 18S rRNA FAM/MGB Probe (Applied Biosystems) was used as the endogenous control. Amplifications were performed as described already. For clinical correlation, patients were linked to a provincial laboratory database (AKDN[34]), and outpatient serum creatinine measurements within 6 months of the biopsy date were retrieved. Baseline kidney function was defined by the serum creatinine measurement closest to the biopsy date. Patients ($n = 4$) with serum creatinine level >300 μmol/L

were excluded from the analysis to avoid patients with ESRD. The association between serum creatinine and NLRP3 mRNA expression (log-transformed because of its skewed distribution) was evaluated using Pearson correlation coefficient.

Semiquantitative reverse transcriptase PCR for mouse and human NLRP3 mRNA expression was performed as already described with the exception of the PCR reaction. These were conducted using 100 ng of cDNA, 500 nM oligonucleotides, 1.25 U of Taqpolymerase (Qiagen), dNTPs (100 μM each), and reaction buffer in a final volume of 25 μl. Reactions were performed using an MJ Research PTC-100 thermal cycler with denaturation 94°C, annealing at 58°C, and extension at 72°C, for a total of 30 cycles. PCR products were separate by electrophoresis on 1% agarose gels.

Histology and Immunohistochemistry

Paraffin-embedded kidney tissues were sectioned and stained with Masson trichrome and hematoxylin and eosin using standard protocols. TUNEL staining on paraffin-embedded kidney sections was performed using the In Situ Cell Death Detection Kit as per the manufacturer's protocol (Roche). TUNEL-positive cells were quantified by counting and averaged over five random fields of view ($\times$40). CD11b immunohistochemistry was performed on acetone-fixed frozen kidney sections using rat anti-mouse CD11b antibody (Mac-1; BD Pharmingen). Rabbit anti-rat IgG was used as the secondary followed by staining with the ABC protocol and DAB substrate (Vector Laboratories). Histologic and immunohistochemical images were captured with a Qcolor5 Olympus camera attached to an Olympus BX51 light microscope along with QCapturePro 6.0 software. Five high-resolution images of the renal cortex were randomly captured with a $\times$20 magnification objective lens. Image analysis was carried out using the Volocity X64 software. Fibrosis area in Masson trichrome slides was quantified by determining the number of pixels present in distinct areas of blue staining compared with the total number of pixels present in the field of view. Pixel values from the five images were averaged to a final value and expressed as percentage area. Leukocyte infiltrate area in CD11b-stained slides were analyzed in the same manner with dark tan and brown pixels examined. Esterase staining was performed on paraffin-embedded tissues as described previously.[44] F4/80 immunofluorescence was performed using a biotinylated rat anti-mouse F4/80 antibody (clone A3-1; Serotec) and Cy2-conjugated avidin for imaging.

Pathology scoring for tubular injury was performed in a blinded manner on hematoxylin- and eosin-stained slides by two individuals independently. Tubular injury was assessed in sections using a semiquantitative scale in which the percentage of cortical tubular necrosis was assigned a score as follows: 0 = normal; 1 = $<$20%; 2 = 20 to 40%; 3 = 40 to 60%; 4 = 60 to 80%; and 5 = 80%. Quantification of tubular injury was performed using the Volocity X64 software as already described. Noninjured, nondilated cortical tubules were selected from the kidney section using the same criteria as pathologic scoring. Intact tubular area was determined by the total number of selected pixels converted to area in mm^2.

Statistical Analysis

Statistical analyses were performed using GraphPad Instat software. All data were expressed as mean $\pm$ SD. The results were analyzed for statistical variance using an unpaired *t* test or one-way ANOVA as appropriate. Nonparametric data were analyzed using the Mann-Whitney *U* test. Results were considered statistically significant at $P < 0.05$. All human studies were conducted with the approval of the Conjoint Health Research Ethics Board at the University of Calgary.

ACKNOWLEDGMENTS

This study was supported by operating grants from the Canadian Institutes for Health Research and infrastructure grants from the Canadian Foundation for Innovation. D.A.M., P.L.B., and B.H. are recipients of Alberta Heritage Foundation for Medical Research Independent Investigator Awards. D.A.M. holds a Tier II Canada Research Chair. B.H. holds a New Investigator Award from the Canadian Institutes of Health Research. S.H. is the recipient of Alberta Heritage Foundation for Medical Research Postdoctoral Fellowship Award.

DISCLOSURES

D.A.M. and P.L.B. have an ownership interest in Arch Biopartners Inc.

REFERENCES

1. Collins AJ, Foley RN, Gilbertson DT, Chen SC: The state of chronic kidney disease, ESRD, and morbidity and mortality in the first year of dialysis. *Clin J Am Soc Nephrol* 4[Suppl 1]: S5–S11, 2009
2. US Renal Data System: *USRDS 2009 Annual Data Report: Atlas of End-Stage Renal Disease in the United States*, Bethesda, National Institutes of Health, National Institute of Diabetes and Digestive and Kidney Diseases, 2009
3. Morii T, Fujita H, Narita T, Koshimura J, Shimotomai T, Fujishima H, Yoshioka N, Imai H, Kakei M, Ito S: Increased urinary excretion of monocyte chemoattractant protein-1 in proteinuric renal diseases. *Ren Fail* 25: 439–444, 2003
4. Mezzano SA, Droguett MA, Burgos ME, Ardiles LG, Aros CA, Caorsi I, Egido J: Overexpression of chemokines, fibrogenic cytokines, and myofibroblasts in human membranous nephropathy. *Kidney Int* 57: 147–158, 2000
5. Grandaliano G, Gesualdo L, Bartoli F, Ranieri E, Monno R, Leggio A, Paradies G, Caldarulo E, Infante B, Schena FP: MCP-1 and EGF renal expression and urine excretion in human congenital obstructive nephropathy. *Kidney Int* 58: 182–192, 2000
6. Ricardo SD, van Goor H, Eddy AA: Macrophage diversity in renal injury and repair. *J Clin Invest* 118: 3522–3530, 2008
7. Johnson RJ: Cytokines, growth factors and renal injury: Where do we go now? *Kidney Int Suppl* 63: S2–S6, 1997
8. Lange-Sperandio B, Trautmann A, Eickelberg O, Jayachandran A, Oberle S, Schmidutz F, Rodenbeck B, Homme M, Horuk R, Schaefer F: Leukocytes induce epithelial to mesenchymal transition after unilateral ureteral obstruction in neonatal mice. *Am J Pathol* 171: 861–871, 2007
9. Liu Y: Epithelial to mesenchymal transition in renal fibrogenesis: Pathologic significance, molecular mechanism, and therapeutic intervention. *J Am Soc Nephrol.* 15: 1–12, 2004

10. Gobe G, Willgoss D, Hogg N, Schoch E, Endre Z: Cell survival or death in renal tubular epithelium after ischemia-reperfusion injury. *Kidney Int* 56: 1299–1304, 1999
11. Rovere-Querini P, Capobianco A, Scaffidi P, Valentinis B, Catalanotti F, Giazzon M, Dumitriu IE, Muller S, Iannacone M, Traversari C, Bianchi ME, Manfredi AA: HMGB1 is an endogenous immune adjuvant released by necrotic cells. *EMBO Rep* 5: 825–830, 2004
12. Shi Y, Zheng W, Rock KL: Cell injury releases endogenous adjuvants that stimulate cytotoxic T cell responses. *Proc Natl Acad Sci U S A* 97: 14590–14595, 2000
13. Ishii KJ, Suzuki K, Coban C, Takeshita F, Itoh Y, Matoba H, Kohn LD, Klinman DM: Genomic DNA released by dying cells induces the maturation of APCs. *J Immunol* 167: 2602–2607, 2001
14. Ting JP, Lovering RC, Alnemri ES, Bertin J, Boss JM, Davis BK, Flavell RA, Girardin SE, Godzik A, Harton JA, Hoffman HM, Hugot JP, Inohara N, Mackenzie A, Maltais LJ, Nunez G, Ogura Y, Otten LA, Philpott D, Reed JC, Reith W, Schreiber S, Steimle V, Ward PA: The NLR gene family: A standard nomenclature. *Immunity* 28: 285–287, 2008
15. Yamamoto S, Ma X: Role of Nod2 in the development of Crohn's disease. *Microbes Infect* 11: 912–918, 2009
16. Martinon F, Mayor A, Tschopp J: The inflammasomes: Guardians of the body. *Annu Rev Immunol* 27: 229–265, 2009
17. Agostini L, Martinon F, Burns K, McDermott MF, Hawkins PN, Tschopp J: NALP3 forms an IL-1beta-processing inflammasome with increased activity in Muckle-Wells autoinflammatory disorder. *Immunity* 20: 319–325, 2004
18. Martinon F, Burns K, Tschopp J: The inflammasome: A molecular platform triggering activation of inflammatory caspases and processing of proIL-beta. *Mol Cell* 10: 417–426, 2002
19. Zhou R, Tardivel A, Thorens B, Choi I, Tschopp J: Thioredoxin-interacting protein links oxidative stress to inflammasome activation. *Nat Immunol* 11: 136–140, 2010
20. Martinon F, Petrilli V, Mayor A, Tardivel A, Tschopp J: Gout-associated uric acid crystals activate the NALP3 inflammasome. *Nature* 440: 237–241, 2006
21. Muruve DA, Petrilli V, Zaiss AK, White LR, Clark SA, Ross PJ, Parks RJ, Tschopp J: The inflammasome recognizes cytosolic microbial and host DNA and triggers an innate immune response. *Nature* 452: 103–107, 2008
22. Mariathasan S, Weiss DS, Newton K, McBride J, O'Rourke K, Roose-Girma M, Lee WP, Weinrauch Y, Monack DM, Dixit VM: Cryopyrin activates the inflammasome in response to toxins and ATP. *Nature* 440: 228–232, 2006
23. Yamasaki K, Muto J, Taylor KR, Cogen AL, Audish D, Bertin J, Grant EP, Coyle AJ, Misaghi A, Hoffman HM, Gallo RL: NLRP3/cryopyrin is necessary for interleukin-1beta (IL-1beta) release in response to hyaluronan, an endogenous trigger of inflammation in response to injury. *J Biol Chem* 284: 12762–12771, 2009
24. Babelova A, Moreth K, Tsalastra-Greul W, Zeng-Brouwers J, Eickelberg O, Young MF, Bruckner P, Pfeilschifter J, Schaefer RM, Groene HJ, Schaefer L: Biglycan: A danger signal that activates the NLRP3 inflammasome *via* toll-like and P2X receptors. *J Biol Chem* 284: 24035–24048, 2009
25. Dostert C, Petrilli V, Van Bruggen R, Steele C, Mossman BT, Tschopp J: Innate immune activation through Nalp3 inflammasome sensing of asbestos and silica. *Science* 320: 674–677, 2008
26. Imaeda AB, Watanabe A, Sohail MA, Mahmood S, Mohamadnejad M, Sutterwala FS, Flavell RA, Mehal WZ: Acetaminophen-induced hepatotoxicity in mice is dependent on Tlr9 and the Nalp3 inflammasome. *J Clin Invest* 119: 305–314, 2009
27. Jones LK, O'Sullivan KM, Semple T, Kuligowski MP, Fukami K, Ma FY, Nikolic-Paterson DJ, Holdsworth SR, Kitching AR: IL-1RI deficiency ameliorates early experimental renal interstitial fibrosis. *Nephrol Dial Transplant* 24: 3024–3032, 2009
28. Vesey DA, Cheung C, Cuttle L, Endre Z, Gobe G, Johnson DW: Interleukin-1beta stimulates human renal fibroblast proliferation and matrix protein production by means of a transforming growth factor-beta-dependent mechanism. *J Lab Clin Med* 140: 342–350, 2002
29. Bani-Hani AH, Leslie JA, Asanuma H, Dinarello CA, Campbell MT, Meldrum DR, Zhang H, Hile K, Meldrum KK: IL-18 neutralization ameliorates obstruction-induced epithelial-mesenchymal transition and renal fibrosis. *Kidney Int* 76: 500–511, 2009
30. Vesey DA, Cheung CW, Cuttle L, Endre ZA, Gobe G, Johnson DW: Interleukin-1beta induces human proximal tubule cell injury, alpha-smooth muscle actin expression and fibronectin production. *Kidney Int* 62: 31–40, 2002
31. Wu H, Chen G, Wyburn KR, Yin J, Bertolino P, Eris JM, Alexander SI, Sharland AF, Chadban SJ: TLR4 activation mediates kidney ischemia/reperfusion injury. *J Clin Invest* 117: 2847–2859, 2007
32. Lee HT, Kim M, Jan M, Penn RB, Emala CW: Renal tubule necrosis and apoptosis modulation by A1 adenosine receptor expression. *Kidney Int* 71: 1249–1261, 2007
33. Mullen P: PARP cleavage as a means of assessing apoptosis. *Methods Mol Med* 88: 171–181, 2004
34. Hemmelgarn BR, Clement F, Manns BJ, Klarenbach S, James MT, Ravani P, Pannu N, Ahmed SB, MacRae J, Scott-Douglas N, Jindal K, Quinn R, Culleton BF, Wiebe N, Krause R, Thorlacius L, Tonelli M: Overview of the Alberta Kidney Disease Network. *BMC Nephrol* 10: 30, 2009
35. Iyer SS, Pulskens WP, Sadler JJ, Butter LM, Teske GJ, Ulland TK, Eisenbarth SC, Florquin S, Flavell RA, Leemans JC, Sutterwala FS: Necrotic cells trigger a sterile inflammatory response through the Nlrp3 inflammasome. *Proc Natl Acad Sci U S A* 106: 20388–20393, 2009
36. Bauernfeind FG, Horvath G, Stutz A, Alnemri ES, MacDonald K, Speert D, Fernandes-Alnemri T, Wu J, Monks BG, Fitzgerald KA, Hornung V, Latz E: Cutting edge: NF-kappaB activating pattern recognition and cytokine receptors license NLRP3 inflammasome activation by regulating NLRP3 expression. *J Immunol* 183: 787–791, 2009
37. Shao W, Yeretssian G, Doiron K, Hussain SN, Saleh M: The caspase-1 digestome identifies the glycolysis pathway as a target during infection and septic shock. *J Biol Chem* 282: 36321–36329, 2007
38. Chevalier RL, Forbes MS, Thornhill BA: Ureteral obstruction as a model of renal interstitial fibrosis and obstructive nephropathy. *Kidney Int* 75: 1145–1152, 2009
39. Li H, Ambade A, Re F: Cutting edge: Necrosis activates the NLRP3 inflammasome. *J Immunol* 183: 1528–1532, 2009
40. Goncalves RG, Gabrich L, Rosario A Jr, Takiya CM, Ferreira ML, Chiarini LB, Persechini PM, Coutinho-Silva R, Leite M Jr: The role of purinergic P2X7 receptors in the inflammation and fibrosis of unilateral ureteral obstruction in mice. *Kidney Int* 70: 1599–1606, 2006
41. Taylor KR, Yamasaki K, Radek KA, Di Nardo A, Goodarzi H, Golenbock D, Beutler B, Gallo RL: Recognition of hyaluronan released in sterile injury involves a unique receptor complex dependent on Toll-like receptor 4, CD44, and MD-2. *J Biol Chem* 282: 18265–18275, 2007
42. White LR, Blanchette JB, Ren L, Awn A, Trpkov K, Muruve DA: The characterization of alpha5-integrin expression on tubular epithelium during renal injury. *Am J Physiol Renal Physiol* 292: F567–F576, 2007
43. Beck PL, Li Y, Wong J, Chen CW, Keenan CM, Sharkey KA, McCafferty DM: Inducible nitric oxide synthase from BM-derived cells plays a critical role in regulating colonic inflammation. *Gastroenterology* 132: 1778–1790, 2007
44. Muruve DA, Barnes MJ, Stillman IE, Libermann TA: Adenoviral gene therapy leads to rapid induction of multiple chemokines and acute neutrophil-dependent hepatic injury *in vivo*. *Hum Gene Ther* 10: 965–976, 1999